Adsorption (2014) 20:935–943
DOI 10.1007/s10450-014-9638-4

Carboxylic acid recovery from aqueous solutions by activated carbon produced from sugarcane bagasse

Erika Suescún-Mathieu · Andrea Bautista-Carrizosa · Rocio Sierra · Liliana Giraldo · Juan Carlos Moreno-Piraján

Received: 26 June 2014 / Revised: 6 September 2014 / Accepted: 9 September 2014 / Published online: 20 September 2014

Abstract This work explores the use of activated carbon (AC) synthesized from sugarcane bagasse (SB) to adsorb volatile carboxylic acids (VCA). Activation was performed by impregnation of SB with 20 and 35 % v/v H_3PO_4 (resulting P20 and P35 respectively) and by impregnation with 30 and 40 % v/v $ZnCl_2$ (resulting Zn30 and Zn40 respectively). Since a low adsorption of VCA was expected in acid activated carbons, they were modified with KOH resulting P20 K and P35 K. Characterization of the produced ACs showed essentially microporous carbons, and points of zero charge between 8.4 and 9.2 that favor chemisorption of anions as VCA carboxylates. Zn40 showed the highest individual VCA molar adsorption percentages, followed by P35 K which also showed a highly microporous surface and sites of high adsorption energy on the N_2 adsorption isotherms. Desorption by sonication and heating was performed on Zn40 after acetic acid adsorption, obtaining the highest desorption percentage by sonication.

Keywords Activated carbon · Sugarcane bagasse · Chemical activation · Volatile carboxylic acids

E. Suescún-Mathieu · A. Bautista-Carrizosa · R. Sierra
Departamento de Ingeniería Química, Universidad de los Andes, Carrera 1 No. 18 A-10, Bogotá, DC, Colombia

L. Giraldo
Departamento de Química, Facultad de Ciencias, Universidad Nacional de Colombia, Carrera 30 No. 45-03, Bogotá, DC, Colombia

J. C. Moreno-Piraján (✉)
Departamento de Química, Grupo de Investigación en Sólidos Porosos y Calorimetría, Facultad de Ciencias, Universidad de los Andes, Carrera 1 No. 18 A-10, Bogotá, DC, Colombia
e-mail: jumoreno@uniandes.edu.co

1 Introduction

Due to the discovery of huge petroleum deposits, the price of gasoline and diesel has been low for decades. However, the increase in these prices, the global warming, and the need to produce fuels from renewable sources, have boosted the investigation on mechanisms for biofuels production. In the MixAlco™ process (Holtzapple et al. 1999; Holtzapple et al. 2011), biomass is pretreated to enhance digestibility, and then it is anaerobically fermented using a naturally occurring mixed culture of acid-forming microorganisms (see Fig. 1). A buffer (e.g. $CaCO_3$ or NH_4HCO_3) is added to neutralize the produced acids, and the resulting carboxylate salts solution is concentrated. The concentrated carboxylate salts can be chemically converted to a variety of chemicals (ketones, carboxylic acids, esters and ethers) and fuels (primary alcohols, secondary alcohols, and gasoline) (Aiello-Mazzarri et al. 2006).

During the acid springing stage of the MixAlco™ process, a thermal conversion of the carboxylic salts mixture (which results from fermentation) into the corresponding VCA takes place (see Fig. 2). Depending on fermentation conditions, VCA content and composition after acid springing may vary widely; however, VCA solutions in concentrations close to 20 % (v/v) containing acetic acid (in the highest concentrations) and small proportions of propionic and butiric acids have been observed (Saad et al. 2010). In order to separate the VCA, which are to be chemically treated in subsequent steps, adsorption in AC is considered as an economically advantageous alternative to other techniques, such as distillation (Amin 2008).

Aiming to explore the application of AC into the MixAlco™, the present study focused on the synthesis of carbons from SB, their activation with H_3PO_4 and $ZnCl_2$, characterization, and use for adsorption of VCA. Figure 3

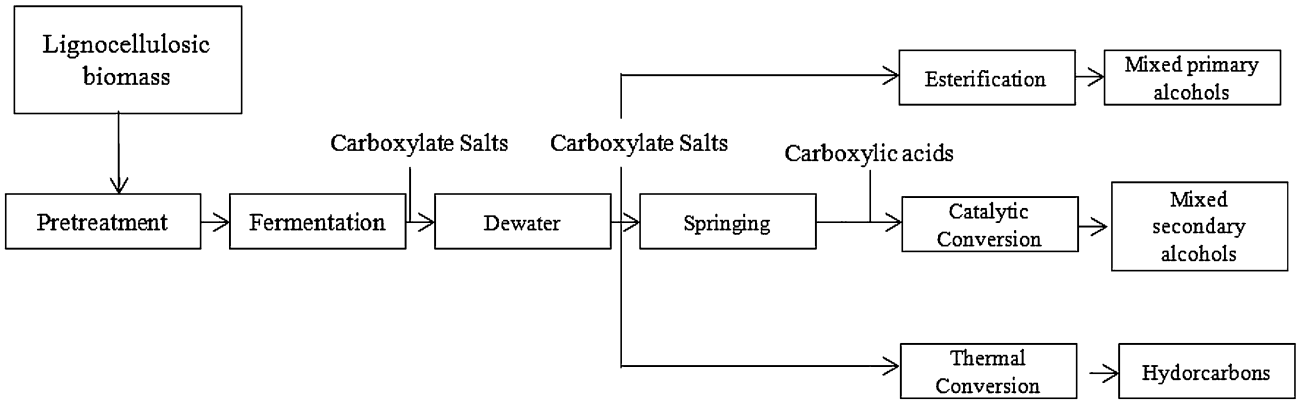

Fig. 1 Overall MixAlco™ process (Aiello-Mazazarri et al. 2006)

Fig. 2 Acid springing step in the MixAlco™ process. Adapted from Aiello-Mazazarri et al. (2006)

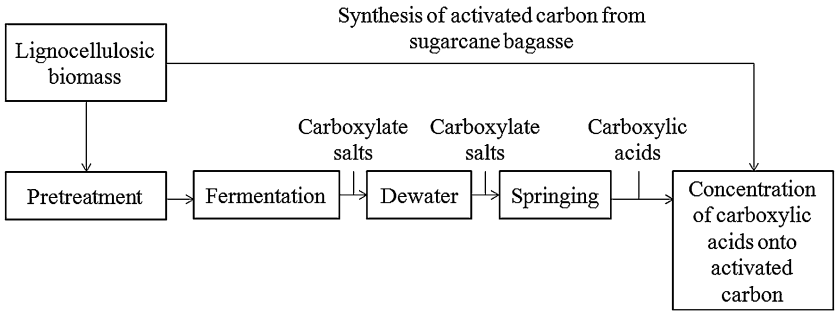

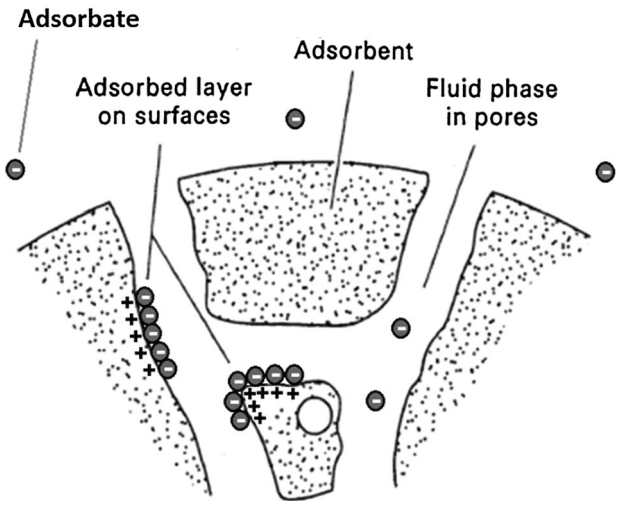

Fig. 3 Chemisorption of VCA carboxylates on AC. Adapted from Seader and Henley (2006)

shows a schematic representation of a proposed chemisorption mechanism. Because VCA are to be chemically converted during the MixAlco™ process, desorption of the adsorbed VCA through sonication and heating was explored.

SB was chosen as the raw material for the synthesis of AC given its high availability, low cost, low inorganic matter content, ease of activation, and low degradation upon storage after appropriate drying (Marsh and Rodríguez-Reinoso 2006). It is a fibrous lignocellulosic material, which is obtained as a residue after sugarcane stalks undergo a juice extraction process. It represents about 25 % of the sugarcane, has an approximate content of 50 % cellulose, 25 % hemicellulose, and 25 % lignin (Gusmão et al. 2012; Vargas et al. 2012), and it is primarily intended to replace fossil fuels in industrial sugar mill operations (Ravelo-Ron et al. 2002). In Colombia, not all of SB is used and of the total production, about 15 % is considered as a residue. According to the Statistics Division of the Food and Agriculture Organization of the United Nations (FAOSTAT), in 2011 Colombia was ranked as the thirteenth largest producer of sugarcane in the world, with a production close to 23 million tonnes valued at nearly 750,000 thousand dollars. As a result, Colombia produces approximately 850,000 tonnes per year of residual SB. This waste material has a high potential for becoming a value added product, such as AC.

2 Methods

2.1 AC synthesis

SB obtained from sugarcane plantations located in the northeast of Colombia (Hoya del Río Suárez) was placed in

a MERMMET UFB 700 oven at 318 K for two weeks. After reaching a moisture content lower than 10 %, the SB was grinded (knife mill) and sieved to pass Tyler mesh 40.

50 g of the recovered fraction, were taken for activations using the following impregnation reagents: 20 % v/v H_3PO_4, 35 % v/v H_3PO_4, 30 % v/v $ZnCl_2$, and 40 % v/v $ZnCl_2$. The obtained AC samples were labeled P20, P35, Zn30, and Zn40 respectively. For activation, the impregnated samples were placed in a LINDBERG/BLUE Gravity One oven at 353 K for three days, and then placed in a Carbolite 1009 furnace at 1,123 K for 4 h, using a temperature ramp of 10 K min^{-1} in an inert atmosphere (N_2). In order to remove excess zinc salts, 50 mL of 0.1 M HCl were added to Zn30 and Zn40. The mixture was stirred at 100 rpm until boiling was observed; afterwards, Zn30 and Zn40 were recovered by vacuum filtration and then, all AC samples were washed with deionized water in a Soxhlet until reaching a constant pH. Because the chemical affinity of the acid activated carbons for the VCA was expected to be low, their surface chemistry was modified by adding 100 mL of KOH at 40 % v/v to 10 g of AC, after which the samples were placed in an incubator at 343 K for 2 h. The samples were agitated in a shaker at 308 K for 24 h, and then washed with deionized water in a Soxhlet until reaching a constant pH. The alkine-modified samples were labeled P20 K and P35 K respectively. Finally, the four AC samples were dried in a MERMMET UFB 500 oven at 353 K for 24 h.

2.2 AC characterization

2.2.1 Textural characterization

The surface physical properties of the obtained AC samples, were determined by nitrogen adsorption at 77 K on a Quantachrome ASi Qwin-Au equipment. The surface area (S) was calculated using the BET model, the micropore volume (V_o) was obtained by applying the Dubinin-Radushkevich model to the adsorption data, and the total pore volume was also calculated (Sing et al. 1985). The pore size distribution was calculated using the Dubinin-Astakov model at low pressures, for values of $P/P^0 < 0.1$, and using the BJH method with Boer distribution at high pressures, for values of $P/P^0 > 0.35$.

2.2.2 Surface chemistry characterization

For the Boehm method, 50 mL of 0.1 M solutions of $NaHCO_3$, Na_2CO_3, NaOH and HCl were prepared and standardized. 0.1 g of AC were suspended in these solutions for six days, and then they were titrated to determine the surface functional groups (Boehm 2002; Boehm et al. 1966). For the point of zero charge (PZC) different amounts of the AC samples, ranging from 0 to 0.6 g, were weighed and placed in a 30 mL flask with 10 mL of a 0.1 M NaCl solution. The bottles were capped and stirred at 298 K for 3 days, and then the pH of each solution was measured (Chan et al. 2011).

2.3 VCA adsorption

To study the capability of the AC samples to adsorb single VCAs in solutions at a concentration of 20 % v/v, 100 mL of the following solutions in water were prepared: Acetic acid, propionic acid, and butyric acid. 1 g of each one of the four types of AC was added to each one of these solutions, and then an aliquot of the solution was taken every 12 h during a 3 day period. These aliquots were analyzed through gas chromatography to determine the adsorption capacity as had been done in previous studies (López et al. 2014).

Additionally, solutions of VCA mixtures containing acetic acid at 16 % v/v, propionic acid at 2 % v/v and butyric acid at 2 % v/v were prepared to conduct competitive adsorption tests. The sampling and analysis procedure used in the single VCA solutions was also applied to the solutions of VCA mixtures for each one of the four AC samples.

2.4 Desorption tests

Four different desorption tests were performed to selected AC samples after adsorption (only those showing the highest VCA adsorption). The implemented techniques were sonication (S), heating (H), sonication followed by heating (S + H) and, finally, heating followed by sonication (H + S). Sonication was performed using a Sonics & Materials Inc. VCX-756 tip sonicator, which operates for 20 s and stops for 40 s per minute. It was applied to samples placed in a falcon containing 1 g of AC and 5 mL of deionized water for 35 min. Heating was carried out in a Barnstead/Labline SHKE7000 incubator at 333 K for 24 h using the same amounts of AC and deionized water in a closed flask. An aliquot of the resulting solutions was taken, filtrated, and submitted to a chromatographic analysis in order to determine the amount of desorbed VCA.

2.5 Scanning electron microscopy (SEM)

It was performed using a JEOL JSM-649OLV SEM, to reveal the morphology and superficial structures of the ACs and the SB. It is a useful tool to observe the particle surface and the extension of the pores.

Table 1 Surface functional groups concentration for SB and AC samples and pH_{PZC} values

Sample	pH_{PZC}	Functional groups concentration (μmol g^{-1})				
		Carboxyl	Lactonic	Fenolic	Acid	Basic
SB	8.3	68.6	29.4	107.8	205.8	29.4
Zn30	8.4	49.0	19.6	93.1	161.7	181.3
Zn40	8.7	39.2	19.6	83.3	142.1	196.0
P20K	8.5	34.3	14.7	78.4	127.4	220.5
P35K	9.2	19.6	9.8	68.6	98.0	269.5

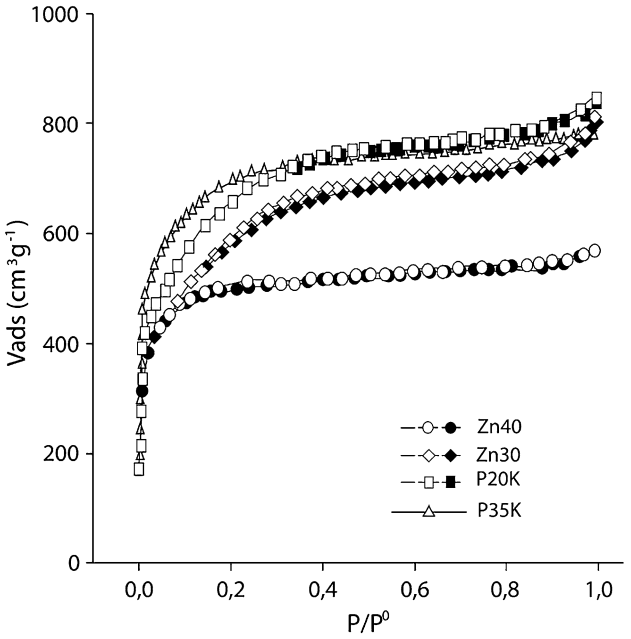

Fig. 4 N_2 adsorption and desorption isotherms at 77 K for AC samples

3 Results and discussion

3.1 Surface chemistry

The surface chemistry of the AC samples was analyzed by the Boehm method. Table 1 shows the surface functional groups of the AC samples in relation to the values of pH_{PZC}. These results show that activating with $ZnCl_2$ acts as a Lewis acid, which could be interpreted as enhancing the aromatic condensation reactions by facilitating the evolution of molecular hydrogen from the hydroaromatic structure of the precursor and, thereby, leaving some active sites on adjacent molecules that can undergo aromatization (polymerization) reactions. Modifying the H_3PO_4 AC with KOH, leads to a slight enrichment in surface basic groups and, therefore, increases the pH_{PZC}. At a pH lower than these pH_{PZC} values, the AC surface exhibited a net positive charge, promoting the chemisorption of anions such as VCA carboxylates to produce VCA salts. Given that all the pH_{PZC} obtained are basic, VCA carboxylates adsorption is favored.

3.2 N_2 adsorption isotherms

The nitrogen adsorption and desorption isotherms for the four AC samples, are presented in Fig. 4. Regardless of the activation procedure, the data obtained for all AC samples adjust to a type I isotherm, indicating that the produced ACs are microporous solids (Sing et al. 1985). The adsorbed amount of adsorbate increases with the relative pressure, until reaching a final value corresponding to the total coverage of the surface with an adsorbate monolayer.

The adsorption at the initial part of the isotherm, at P/P^0 values from zero to about 0.05, is an indicative of the microporosity dimensions such that the steeper the gradient, the narrower the micropores. Based on this, P35 K followed by P20 K have the narrower pores among the studied AC samples. The initial part of the isotherm, at values of $P/P^0 << 0.001$, indicates the presence of sites of high adsorption energy (Marsh and Rodríguez-Reinoso 2006), which are slightly more visible for the P35 K isotherms. Given that activated carbons in industrial applications need to adsorb at low relative pressures in gas phase, and taking into account the highly microporous surface, small pore size, and sites of high adsorption energy of P35 K, it is profiled as a good option for industrial applications.

The shape of the isotherm shows that a substantial quantity of nitrogen is adsorbed at very low pressures, generating a closed shoulder, which, as mentioned above, is characteristic of Type I, isotherms. The obtained ACs

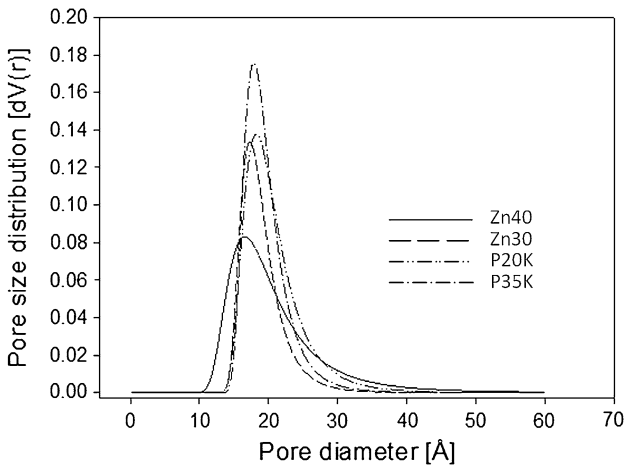

Fig. 5 Comparison of pore size distribution from the isotherms of N_2 adsorption at 77 K

developed a large surface area, which is later associated to the adsorptive capacity of the VCA. This, in conjunction with the apparent area of P35 K (which presented a N_2 adsorption of about 2,200 $cm^3\ g^{-1}$), is an important result of this work, because these features allow for a higher acid recovery capacity than that expected in other types of solids.

Table 2 Textural parameters of the activated carbons. S_{BET} and DA parameters were obtained from the N_2 adsorption isotherm at 77 K

	S_{BET} ($m^2\ g^{-1}$)	DA			
		V_{mic} ($cm^3\ g^{-1}$)	E_0 (kJ mol^{-1})	n	Pore diameter (Å)
Zn40	1617	0.91	4.50	1.40	17.0
Zn30	1997	0.75	4.40	2.80	17.2
P20K	2285	1.05	3.68	2.20	18.2
P35K	2236	1.02	4.00	2.80	17.8

Figure 5 shows the pore distribution of the AC samples. The four AC samples have primarily a pore size distribution below 20 Å; thus, the ACs produced in this study are mainly microporous, as it was previously stated. Likewise, the presence of mesopores is observed, but in such a small degree that adsorption in mesopores is neglected. Instead, mesopores may be considered the entrance to the micropores, where the bulk of the adsorption takes place. P35 K exhibited the largest microporous surface area, followed by P20 K, Zn30 and Zn40 in decreasing order. The activated carbon P35 K also presented the narrower pore size distribution, which will be suitable for the adsorption of VCA. Thus, the higher microporosity content of this solid validates the treatment used during the preparation of the activated carbons.

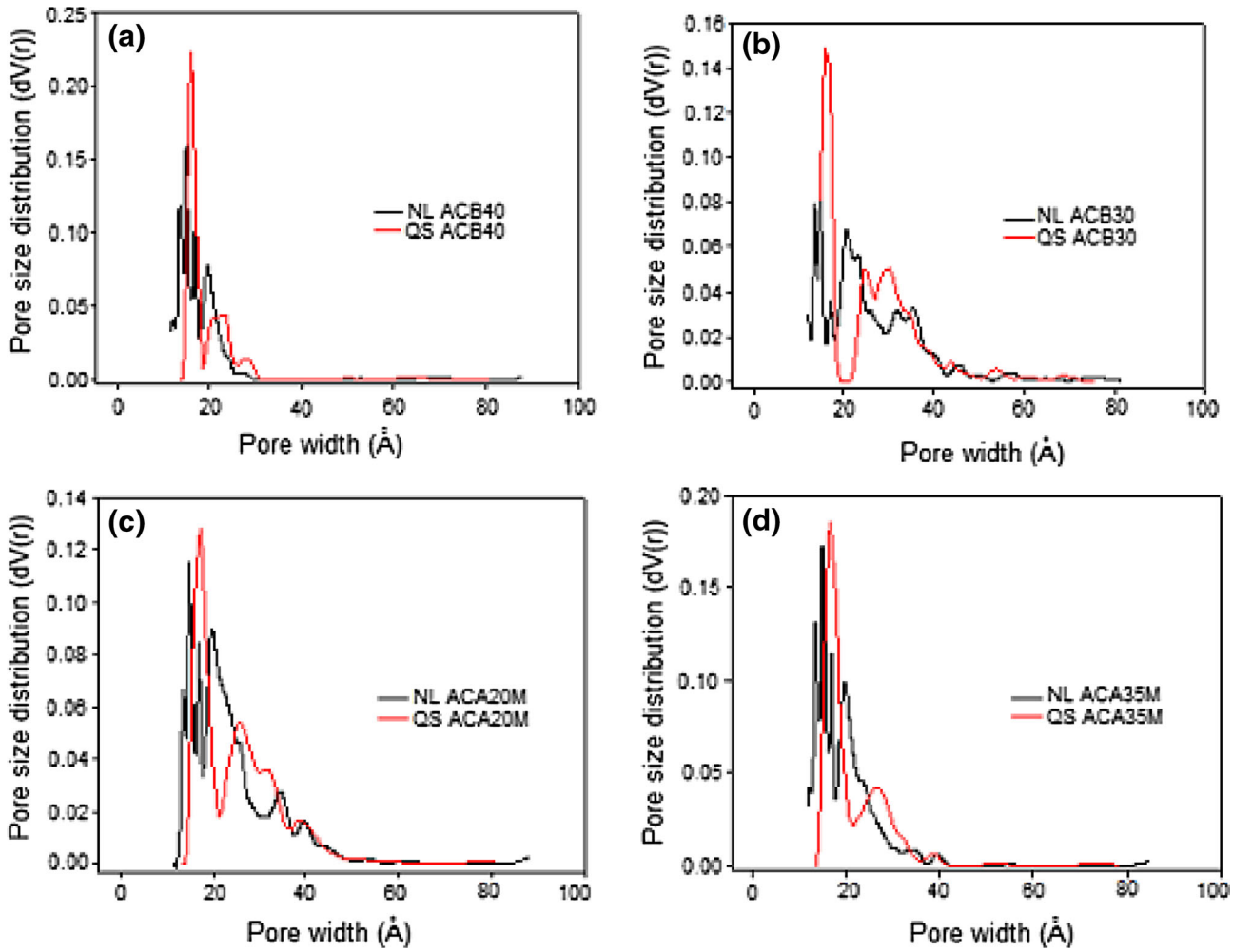

Fig. 6 Pore size distribution of activated carbons according to the data of N_2 adsorption–desorption isotherms at 77 K. **a**) ACB40, **b**) ACB30, **c**) ACA20M, and **d**) ACA35M

In Table 2, the parameter n describes the surface heterogeneity and E describes the adsorption potential; when $n = 2$, the equation of DA reduces to the equation of DR, and when $n < 3$ it describes a heterogeneous system or a system with a broader distribution of pores. The results show that the value of n for three of the activated carbons is greater than 2 for homogeneous micropore distribution from the DR equation. The activated carbon Zn40 presented the lowest value of BET surface area, and it showed the largest pore size distribution according to the value of 1.40 for n and according to Fig. 5. Regarding the characteristic adsorption energy E_0 of the set of activated carbons, values lie between 3.68 and 4.50 kJ mol^{-1}, with lower values for the ACs having a higher adsorption of N_2.

According to the experimental isotherms, the behavior at $P/P^0 < 0.3$ is consistent with the calculations of S_{BET} (in decreasing order, P35 K > P20 K > Zn30 > Zn40). Although Zn40 showed the lowest S_{BET}, it presented the highest energy heterogeneity in the pores distribution at low pressures, with the highest characteristic energy E_0. The analysis using the theory of density functionals, considering homogeneous pore walls (NLDFT), and the effects caused by the presence of heterogeneities (QSDFT), shows a distribution of pores characteristic of heterogeneous microporous solids. Particularly for Zn30 and P20 K, the presence of some differentiated types of mesopores is noticed, which matches with the shape of the experimental adsorption isotherm at $P/P^0 > 0.35$ (the slope of both isotherms increasingly changes in that region) as shown in Fig. 6.

3.3 VCA adsorption

As shown in Table 3, the maximum removal of VCA was obtained in single acid samples since the higher the initial concentration of a single VCA, the higher the percentage thereof adsorbed. The lower percentage of adsorption obtained for the competitive tests, can also be explained by interactions between molecules and ions in the solution that compete for adsorption sites. Zn40 showed the highest individual VCA adsorption percentages. However, individual adsorption percentages for the other AC samples are considerably similar. Also, a higher adsorption percentage was obtained using Zn30 and Zn40 in comparison to P20 K and P35 K. However, by comparing these results with those obtained from the N_2 adsorption isotherms, P20 K and P35 K have a higher volume of micropores than Zn30 and Zn40, and should therefore have a greater capacity for removing VCA from aqueous solutions. This may be explained by the differences in surface functional groups, which promote a higher affinity between $ZnCl_2$ activated samples and VCA, than between H_YPO/KOH samples and VCA. Another possible explanation is an incomplete Soxhlet washing of H_3PO_4/KOH samples after modification, so that the porous surface may be covered with potassium phosphates resulting from the reaction between the impregnating agent (H_3PO_4) and the modifying agent (KOH), thus obstructing the adsorption of VCA but allowing the smaller molecules of N_2 to enter the micropores. In all cases, acetic acid was the adsorbate with the highest adsorption percentages due to its smaller length (approximately 0.3 nm) in comparison to propionic acid (approximately 0.4 nm) and butyric acid (approximately 0.5 nm) (Sutton 1965). This allowed acetic acid molecules to easily move through the micropores and to fill them in a more compact way than the other two adsorbates.

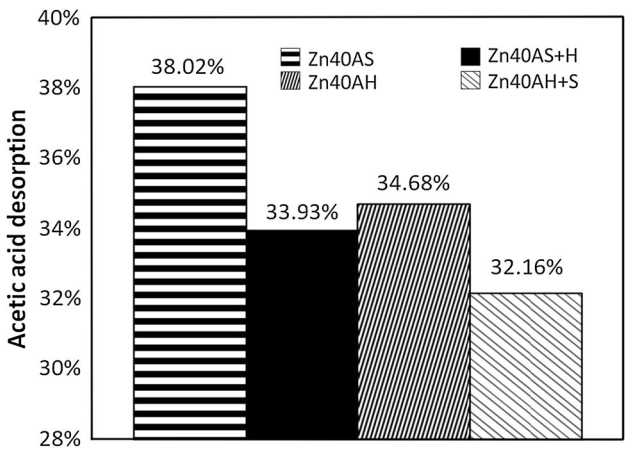

Fig. 7 Acetic acid desorption percentage using different combinations of sonication (*S*) and heating (*H*) on Zn40A

Table 3 Molar adsorption percentages of each AC sample for the individual and competitive adsorption tests

Sample	Individual adsorption test			Competitive adsorption test		
	Acetic acid (%)	Propionic acid (%)	Butyric acid (%)	Acetic acid (%)	Propionic acid (%)	Butyric acid (%)
Zn40	60	48	21	25	2	10
Zn30	56	48	19	26	5	6
P35K	54	46	10	16	12	5
P20K	53	44	10	19	9	9

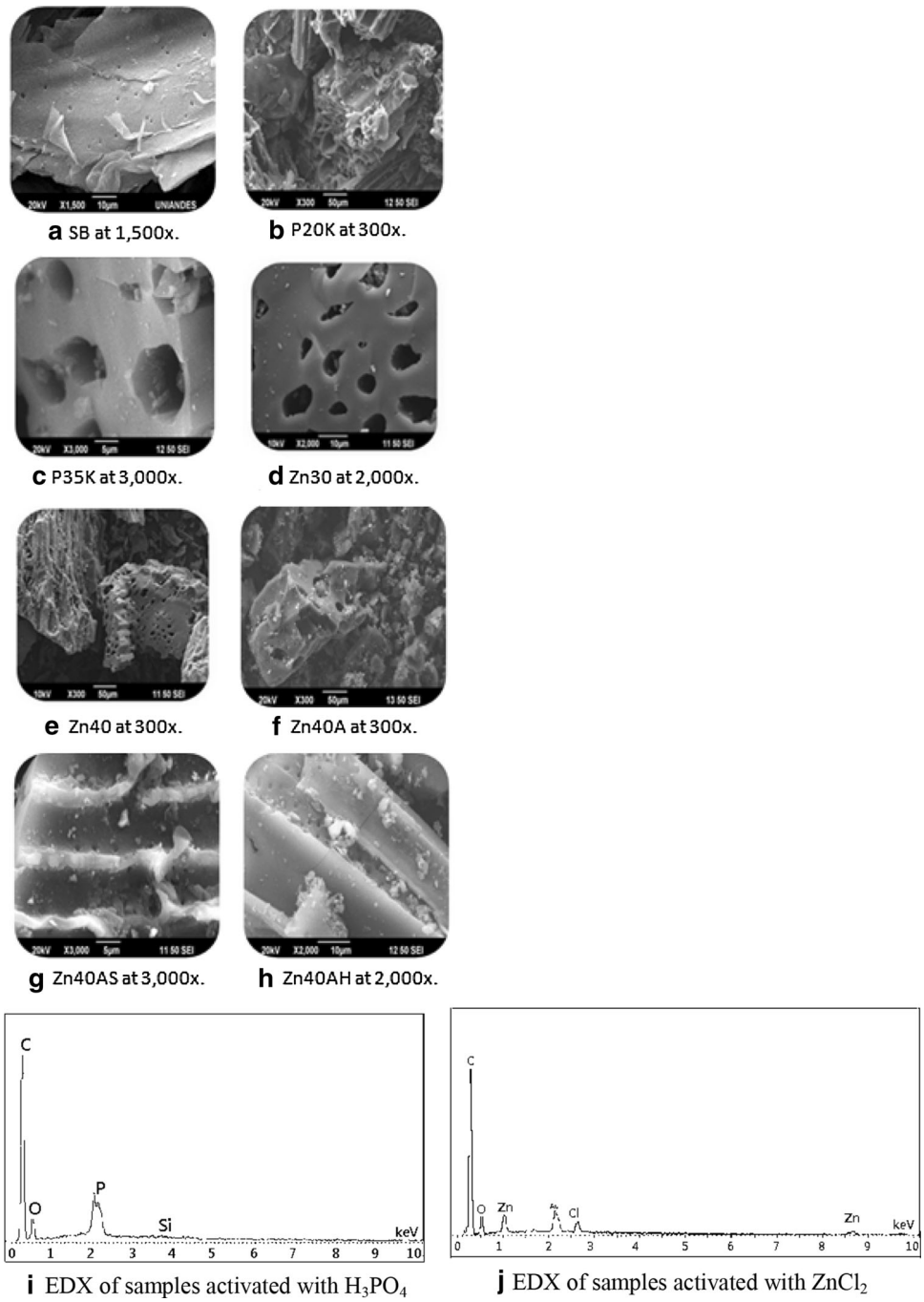

Fig. 8 SEM–EDAX images for the SB and selected AC samples

3.4 Desorption tests

Given that Zn40 exhibited the highest acetic acid adsorption percentage, the sample designated as Zn40A (Zn40 after acetic acid adsorption), was used for the desorption tests consisting on four combinations of sonication and heating: Sonication (S), heating (H), sonication followed by heating (S + H), and heating followed by sonication (H + S). The corresponding desorbed samples were labeled Zn40AS, Zn40AH, Zn40AS + H, Zn40AH + S. Fig. 7 shows the percentage of acetic acid desorption for the four desorption tests applied.

As shown in Fig. 7, the highest VCA desorption percentage was obtained by sonication (Zn40AS), then by heating (Zn40AH), sonication with subsequent heating (Zn40AS + H), and heating with subsequent sonication (Zn40AH + S). However, given the small amount of Zn40A available, the four desorption tests were carried out

without replicas. With this, desorption percentages may not be significantly different from one desorption method to another. According to this, it is recommended to replicate the experiments.

During sonication, ultrasonic waves generate vibrations in the adsorbent and the adsorbate provoking the desorption of the most weakly bound particles, such as those adsorbed by physisorption. However, since most of the VCA was adsorbed by chemisorption, the vibration may not have sufficient energy to break the acid–base bonds in the surface of the AC, so it is suggested to investigate further desorption methods.

3.5 Scanning electron microscopy coupled with energy dispersive X-ray (SEM/EDAX)

Micrographs obtained by SEM-EDAX are shown in Fig. 8, where the change in SB superficial texture and porosity after activation and modification is evidenced.

The micrograph in Fig. 8a shows the layered lignocellulosic structure of SB, where small pores related to the circulatory system of the sugarcane can be seen. The diameter of these pores is of approximately 1 μm, and they can also be seen in Fig. 8g, h. The cavities and fractures are due to the rupture caused by SB pretreatment (Chen et al. 2011). Figure 8b, e, f shows the irregular structure of Zn40 powder particles, which confers it an elevated surface area. In Fig. 8b–f, the porous structure of the AC samples can be seen. The porosity created by $ZnCl_2$ is due to the spaces left by this salt after washing given that it behaves as a template; subsequently, the uniform size of the micropores is due to the small size of the $ZnCl_2$ molecule or its hydrates. This does not happen for H_3PO_4 because there are no phosphoric acid molecules, but a mixture of molecules from the small H_3PO_4 to $H_{13}P_{11}O_{34}$; this leads to heterogeneity in the microporosity of H_3PO_4/KOH samples.

In Fig. 8f small white dots can be seen on the Zn40A surface, which can be attributed to the carboxylic salts that form on the surface of the AC as a result of chemisorption of the acetic acid. In Fig. 8g, h, corresponding to the Zn40A samples with the best desorption results, salts are still observed on the carbon surface, being necessary to employ new desorption techniques to obtain better results. The presence of these salts on the H_3PO_4/KOH samples prior to adsorption (see Fig. 8b, c) can be explained by the reaction between H_3PO_4 and KOH to produce potassium phosphates, which could have remained on the AC surface due to an incomplete Soxhlet washing after modification. The presence of salts on the surface of $ZnCl_2$ activated carbons, may also be due to an incomplete wash of these samples. However, it is of importance to note that the presence of salts on the AC samples before adsorption is low.

Furthermore, energy dispersive X-ray (EDAX) analysis was carried out both in AC samples activated with H_3PO_4 (i.e., P20, P35, P20 K and P35 K) (Fig. 8i) and AC samples activated with $ZnCl_2$ (i.e., Zn30 and Zn40) (Fig. 8j). The data obtained in this way is only a rough estimation (not an absolute determination) of the surface elemental composition. Through these tests, the following elements and composition were found for AC activated with acid: carbon (75.21 %), oxygen (18.61 %), silica (0.2 %) and phosphorus (5.98 %), while for AC activated with zinc chloride the samples were shown to comprise mainly carbon, oxygen and zinc metal, this last compound in a concentration close to 7 %. Both, the phosphate ions and zinc metal come from the reagent (either acid or zinc chloride) used during activation. Moreover, the presence of zinc metal at the carbon surface may be due to the formation of some stable zinc complexes (oxides and carbides), which were not removed during washing with water.

4 Conclusions

The MixAlco^{TM} process is aimed to produce fuels and chemicals from waste biomass through an anaerobic fermentation where acids production is enhanced, followed by downstream chemistry. One important step in MixAlco^{TM} is VCA separation. The use of AC obtained from SB using both H_3PO_4 and $ZnCl_2$ as a impregnating agents, followed by surface modification through exposition to KOH for the acid, shows promising for adsorption of VCA in solutions of low concentration (up to 20 % v/v) of mixtures of acetic, propionic, and butiric acids and for solutions containing only one of these VCA. This application of CA is important to lower energy demands and operating costs in the context of the MixAlco^{TM} process.

During carbon activation following the aforementioned procedure, an enrichment in surface basic groups is achieved thereby increasing the pH_{PZC}. Given that for all AC samples in this study the pH_{PZC} obtained are basic, and that a pH lower than 7 will be obtained at the end of the stage of acidogenic fermentation of the MixAlco^{TM} process, VCA carboxylates adsorption on the ACs is enhanced.

SEM-EDAX micrographs show the irregular and porous structure of AC powder particles, which confers them an elevated surface area. In the micrographs corresponding to the AC samples with the best desorption results (Zn40AS and Zn40AH), salts formed by chemisorption of VCA are still observed in the carbon surface, which makes evident that it is necessary to employ new desorption techniques to obtain better results.

N_2 adsorption isotherms obtained for all AC samples, regardless of the activation procedure, adjust to a type I isotherm, which is exclusive for completely microporous solids, where the absorption takes place in a monolayer. The four AC samples have primarily a pore size distribution below 2 nm; thus, the AC samples produced in this study are mainly microporous. P35 K exhibited the largest microporous surface area, followed by P20 K, Zn30 and Zn40 in decreasing order. P35 K is profiled as a good option for industrial applications in gas phase, due to its highly microporous surface and its sites of high adsorption energy.

Zn40 showed the highest individual VCA adsorption percentages. It was also noticed a higher VCA adsorption percentage by $ZnCl_2$ activated carbons in comparison to the more microporous H_3PO_4/KOH activated carbons, which may be due to an incomplete wash of the H_3PO4/KOH samples after modification, so that the porous surface may be covered with potassium phosphate (K_3PO_4) resulting from the reaction between the impregnating agent (H_3PO_4) and the modifying agent (KOH), thus blocking the adsorption of VCA.

Because the acids are required in downstream processing for the MixAlco^{TM} process, desorption of the VCA from the AC was assessed. The highest VCA desorption percentage was obtained by sonication. However, desorption percentages may not be significantly different, so it is suggested for a future work to replicate the experiment and to investigate further desorption methods that allow the breakage of the bonds formed between the adsorbate and the adsorbent.

Acknowledgments The authors thank the framework Agreement between Universidad de los Andes (Colombia) and Universidad Nacional de Colombia, as well the Agreement Statement (Acta de Acuerdo) between the Departments of Chemistry of both Universities.

References

Aiello-Mazzarri, C., Agbogbo, F.K., Holtzapple, M.T.: Conversion of municipal solid waste to carboxylic acids using a mixed culture of mesophilic microorganisms. Bioresour. Technol. **97**, 47–56 (2006)

Amin, N.K.: Removal of reactive dye from aqueous solutions by adsorption onto activated carbons prepared from sugarcane bagasse pith. Desalination **223**, 152–161 (2008)

Boehm, H.P.: Surface oxides on carbon and their analysis: a critical assessment. In: Eley, D.D., Pines, H., Weisz, P.B., (eds.) Advances in Catalysis, vol. 16, pp. 179–274. Academic Press, New York (1966)

Boehm, H.P.: Surface oxides on carbon and their analysis: a critical assessment. Carbon **40**(2), 145–149 (2002)

Chan, O.S., Cheung, W.H., Mckay, G.: Preparation and characterization of demineralized tyre derived activated carbon. Carbon **49**, 4674–4687 (2011)

Chen, W.H., Tu, Y.J., Sheen, H.K.: Disruption of sugarcane bagasse lignocellulosic structure by means of dilute sulfuric acid pretreatment with microwave-assisted heating. Appl. Energy **88**(8), 2726–2734 (2011)

Gusmão, K.A.G., Gurgel, L.V.A., Melo, T.M.S., Gil, L.F.: Application of succinylated sugarcane bagasse as adsorbent to remove methylene blue and gentian violet from aqueous solutions—kinetic and equilibrium studies. Dyes Pigm. **92**(3), 967–974 (2012)

Holtzapple, M.T., Davison, R.R., Ross, M.K., Aldrett-Lee, S., Nagwani, M., Lee, C.M., Lee, C., Adelson, S., Kaar, W., Gaskin, D., Shirage, H., Chang, N.S., Chang, V.S., Loescher, M.E.: Biomass conversion to mixed alcohol fuels using the MixAlco process. Appl. Biochem. Biotechnol. **77–79**, 609–631 (1999)

Holtzapple, M.T., Davison, R.R., Ross, M.K., Aldrett-Lee, S., Nagwani, M., Lee, C.M., Lee, C., Nachiappana, B., Fu, Z., Holtzapple, M.T.: Ammonium carboxylate production from sugarcane trash using long-term air-lime pretreatment followed by mixed-culture fermentation. Bioresour. Technol. **102**(5), 4210–4421 (2011)

López-Velandia, C., Moreno-Barbosa, J.J., Sierra-Ramirez, R., Giraldo, L., Moreno-Piraján, J.C.: Adsorption of volatile carboxylic acids on activated carbon synthesized from watermelon shell. Adsorpt. Sci. Technol. **32**(2–3), 227–242 (2014)

Marsh, H., Rodríguez-Reinoso, F.: Activated Carbon, pp. 118–129. Elsevier, Amsterdam (2006)

Ravelo-Ron, D., Bermúdez-Savón, R.C., Valiño-Cabrera, E., Pérez-Pardo, J.L.: Fermentación del bagazo de caña de azúcar en un biorreactor a escala de laboratorio. Tecnol. Quím. **22**(2), 32–40 (2002)

Saad, S.A., Isa, K., Bahari, R.: Chemically modified sugarcane bagasse as a potentially low-cost biosorbent for dye removal. Desalination **264**(1–2), 123–128 (2010)

Seader, J.D., Henley, E.J.: Separation Process Principles, 2nd edn. Wiley, New York (2006)

Sing, K.S., Haul, R.A., Pierotti, R.A., Siemieniewska, T.: Reporting physisorption data for gas/solid systems with special reference to the determination of surface area and porosity. Pure Appl. Chem. **57**(4), 603–619 (1985)

Sutton, L.E.: Tables of interatomic distances and configuration in molecules and ions, pp. 1956–1959. The Chemical Society, London (1965). Supplement

Vargas, D.P., Giraldo, L., Moreno Piraján, J.C.: CO_2 adsorption on activated carbon honeycomb-monoliths: a comparison of langmuir and tóth models. J. Mol. Sci. **13**, 8388–8397 (2012)